Love wave propagation in a near-surface depth-varying distribution of cracks

M. Caleap (1), B. W. Drinkwater (1), P. D. Wilcox (1), C. Aristégui (2)

(1) Department of Mechanical Engineering, University of Bristol, Queens Building, University Walk, Bristol BS8 1TR, UK

(2) Université de Bordeaux; CNRS; UMR 5469, Laboratoire de Mécanique Physique, Talence, F-33405, France.

ABSTRACT

Based on a dynamic-homogenization approach, the dispersion spectrum of coherent antiplane waves in an isotropic half-space containing random distribution of strip-like cracks within finite depth beneath the surface is calculated and analyzed. The disorder inside the damaged region is not uniform but depends on depth. The scattering-induced dispersion and attenuation causes the near-surface region to behave as a surface waveguide. As a result, the spectrum resembles that of the Love-waves.

.

INTRODUCTION

The present study is concerned with Love-type (surface) wave propagation in an isotropic half-space containing cracks parallel to the free surface. The cracks are randomly distributed in a region beneath the surface. The disorder inside the damaged region is not uniform as in [1] but depends on depth. The spatial variation of the distribution is taken into account via replacing the damaged region by a stack of effective homogenous transversely isotropic layers [2, 3]. Propagation in each layer is governed by appropriate effective tensors, which are derived by using a dynamic-homogenization approach developed in [4]. The elastic parameters of each layer, associated with the coherent antiplane wave motion, are spatially constant but frequency dependant and complex-valued. The cracks reduce the velocity and thus create a surface waveguide. Frequency dispersion due to the scattering is superposed with that due to the wave trapping beneath the surface. The resultant dispersion spectrum of coherent Love-type waves is calculated in a given half-space and its behaviour discussed. This method might be an effective approach to measure the heterogeneous structure of the Earth's crust.

A LAYER OF CRACKS: EFFECTIVE MEDIUM

Consider a homogeneous, isotropic, and linearly elastic solid containing a random and uniform distribution of identical and parallel strip-like cracks of size $2a$, as shown in Figure 1. All the cracks are infinitely long in the Y axis. The crack faces are stress-free. The number of cracks per unit area (density) is constant and denoted by n.

An incident monochromatic antiplane (shear) wave propagates along the Z axis, normal to the crack faces which coincide with the X axis, Figure 1. The propagation in the crack-free matrix is governed by the wavenumber $k_T = \omega s_T$, where ω is the angular frequency and s_T the slowness of the shear wave in the matrix.
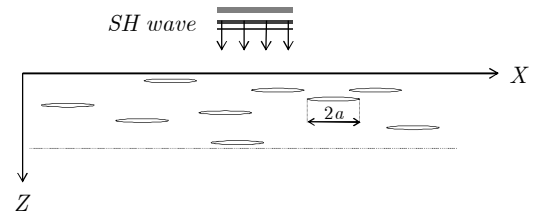
Figure 1. Normally incident antiplane wave on a layer containing a random and uniform distribution of parallel cracks.

It is well known that, in presence of multiple cracks, the coherent plane wave propagation in the damaged medium can be described by a complex-valued wavenumber K. This has been evaluated analytically [4, 5]. The dissipation is assumed to be induced only by the multiple scattering between cracks, *i.e.* the anelastic attenuation is not considered. The coherent shear wave is represented by the displacement components

$$u_x = u_z = 0 \, , \ u_y = U \exp\left(i\omega\left(sz - t \right) \right), \tag{1}$$

where U is an amplitude factor and s $(= K / \omega)$ is the effective slowness that governs antiplane wave propagation in the cracked solid. The equation of motion for the effective material has the form

$$\rho \frac{\partial^2 u_y}{\partial t^2} = \mu \frac{\partial^2 u_y}{\partial z^2}, \tag{2}$$

where ρ is the effective mass density and μ is the effective shear stiffness along the Z axis. Substituting Eq. (1) into Eq. (2), one finds the dispersion relation

$$\rho = \mu s^2 \, . \tag{3}$$

Observe that μ relates linearly the effective stress component σ_{yz} to the effective strain component $\varepsilon_{yz} = \partial u_y / \partial z$.

The dynamic mechanical behaviour of the cracked solid subjected to multiple scattering of shear waves can be described macroscopically by means of both the effective mass density ρ and the effective shear stiffness μ. Due to the geometric arrangement of the crack distribution and the symmetry of the scattered fields, the cracked solid can be seen macroscopically as a transversely isotropic medium. On these grounds, we have found the following relations [2, 4]

$$\rho = \rho_0 \quad \text{and} \quad \mu = \mu_0 \left(1 - n \frac{4\pi}{k_T^2} f(0) \right), \tag{4}$$

where ρ_0 and μ_0 are the mass density and the shear stiffness of the isotropic matrix. The quantity $f(0)$ indicates the far-field response of a single crack in the forward direction with respect to plane-wave excitation propagating normally to the crack faces. The reader is referred to Caleap *et al.* [6] for further details on the derivation of the *forward scattering shape function* $f(\theta)$ for a stress-free strip-like crack.

The effective shear slowness of the coherent wave motion in the direction normal to the crack faces is then obtained by combining Eqs. (3) and (4), *i.e.*

$$s = s_T \left(1 - n \frac{4\pi}{k_T^2} f(0) \right)^{-1}. \tag{5}$$

We recall that the formulae (4) have been derived by viewing the cracked region as a homogeneous *layer* embedded in the matrix. This perspective implies that the bulk parameters (4), and the linear effective constitutive law $\sigma_{yz} = \mu \varepsilon_{yz}$ (involving the spectra of the non-zero stress and strain components, σ_{yz} and ε_{yz}), guarantee the coherent stress vector to be continuous across each interface.

Because the scattering amplitude $f(0)$ is complex-valued, it follows from Eq. (4) that the wave dissipation in the cracked solid is described by the complex-valued effective shear stiffness μ.

As expected, the mass density ρ is equal to that of the matrix: the negligibly small volumes of the cracks do not change the apparent dynamic inertia of the equivalent homogeneous medium. Observe from Eq. (4) that μ depends on the frequency and on the crack density number n.

The phase velocity and the scattering-induced attenuation of the shear bulk waves in the damaged layer can be calculated as follows
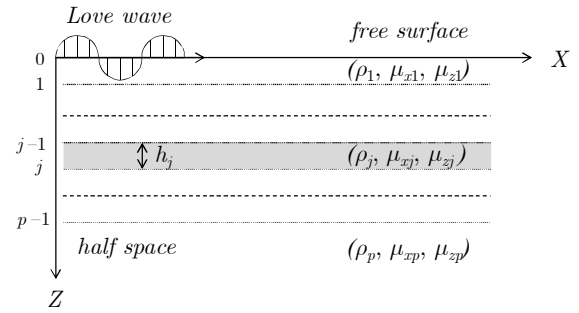
$$c(\omega) = \mathrm{Re}\left(s^{-1}(\omega) \right), \; \alpha(\omega) = \omega \, \mathrm{Im}\, s(\omega). \tag{6}$$

Note that an antiplane wave propagating parallel to the plane of the cracks is not scattered at all. In such case we have

$$\rho = \rho_0, \; \mu = \mu_0 \; \text{and} \; s = s_T. \tag{7}$$

This can also be verified analytically by replacing $f(0)$ in Eqs. (4) and (5) with $f(\pi/2)$, and observing from [6] that $f(\pi/2) = 0$.

The high frequency asymptotic trend of the effective stiffness is [4]

Figure 2. Schematic representation of a multilayered half-space. Each of the $(p-1)$ homogeneous transversely isotropic layers has material parameters $(\rho_j, \mu_{xj}, \mu_{zj})$ and a constant thickness h_j. The pth layer is of semi-infinite extent.

$$\mu(\omega) = \mu_0 \left(1 - \frac{2i}{\omega s_T} \alpha(\infty) \right) \tag{8}$$

i.e., it tends to the matrix value μ_0, whence the effective phase velocity $c(\omega)$ tends to $c_T = s_T^{-1}$ while the effective attenuation $\alpha(\omega)$ approaches a constant value

$$\alpha(\infty) = 2na. \tag{9}$$

DISPERSION SPECTRUM FOR *p*–LAYERS

Consider an elastic half-space composed of p parallel homogeneous and transversely isotropic layers. The pth layer is of semi-infinite extent. The total thickness of the $(p-1)$ layers overlying the half-space is finite and is denoted by H. The geometry under consideration and the numbering of the layers and interfaces is illustrated in Figure 2. The lateral dimensions of the layers are assumed to be infinite. The layer interfaces are horizontal and parallel to the (X, Y) plane. Let $h_j = z_j - z_{j-1}$ be the thickness of the jth layer (z_j being their depth, with the Z axis pointing into the medium). Associated with the jth layer are its effective mass density ρ_j and its effective shear stiffnesses μ_{xj} and μ_{zj} along the X and Z axes. The effective slowness of coherent shear bulk wave in the jth layer satisfies the equation

$$s_j = \sqrt{\frac{\rho_j}{\ell_x^2 \mu_{xj} + \ell_z^2 \mu_{zj}}}, \tag{10}$$

where ℓ_x and ℓ_z are the direction cosines from the X and Z axes. For overall isotropy, $\mu_x = \mu_z = \mu$ and $s = \sqrt{\rho / \mu}$, since $\ell_x^2 + \ell_z^2 = 1$.

The equation of the Love-type motion in the jth layer is

$$\mu_{xj} \frac{\partial^2 u_y}{\partial x_j^2} + \mu_{xj} \frac{\partial^2 u_y}{\partial z_j^2} + \rho_j \omega^2 u_y = 0, \; z_{j-1} < z < z_j. \tag{11}$$

The guided waves are sought of the form

$$u_y(x, z) = \left(A_j e^{i\omega S_{zj} z} + B_j e^{-i\omega S_{zj} z} \right) e^{i(\omega S_x x - \omega t)}, \tag{12}$$

where A_j and B_j are complex-valued amplitudes and

$$S_{zj}^2 = \frac{\mu_{xj}}{\mu_{zj}} \left(s_{xj}^2 - S_x^2 \right). \tag{13}$$

The following technique is similar to that developed by Haskell [7] for simple isotropic layers. Let us introduce the displacement-stress vector

$$\boldsymbol{\mathcal{F}} = \begin{bmatrix} u_y \\ \sigma_{yz} \end{bmatrix}. \tag{14}$$

In the following, we will relate the displacement-stress vectors at the bottom and top interface of each layer. This relation plus the interface and radiation conditions are sufficient to determine motion at depth in terms of the surface conditions. It is immediately realized that $B_p = 0$ to avoid exponential growth with depth, and $B_1 = A_1$ from the traction free surface condition. The other $(2p - 2)$ constants are determined from the interface continuity conditions on displacement and stress.

Taking the origin of Z at the $(j-1)^{th}$ interface we have, at this interface,

$$\boldsymbol{\mathcal{F}}_{j-1} = \begin{bmatrix} A_j + B_j \\ i\omega S_{zj}\mu_{zj}\left(A_j - B_j\right) \end{bmatrix}, \tag{15}$$

and at the jth interface

$$\boldsymbol{\mathcal{F}}_j = \begin{bmatrix} A_j e^{i\omega S_{zj}h_j} + B_j e^{-i\omega S_{zj}h_j} \\ i\omega S_{zj}\mu_{zj}\left(A_j e^{i\omega S_{zj}h_j} - B_j e^{-i\omega S_{zj}h_j}\right) \end{bmatrix}. \tag{16}$$

By eliminating A_j and B_j between Eqs. (15) and (16), we obtain

$$\boldsymbol{\mathcal{F}}_j = m_j\left(\omega, \mu_{zj}, h_j, S_{zj}, S_x\right)\boldsymbol{\mathcal{F}}_{j-1}, \tag{17}$$

where

$$m_j = \begin{bmatrix} \cos\omega S_{zj}h_j & \dfrac{\sin\omega S_{zj}h_j}{\omega S_{zj}\mu_{zj}} \\ -\omega S_{zj}\mu_{zj}\sin\omega S_{zj}h_j & \cos\omega S_{zj}h_j \end{bmatrix}. \tag{18}$$

Equation (18) relates the stress-displacement vectors at the top to that at the bottom of the jth layer. By repeated application, we have

$$\boldsymbol{\mathcal{F}}_{p-1} = \boldsymbol{m}\left(\omega, S_x\right)\boldsymbol{\mathcal{F}}_0, \tag{19}$$

where

$$\boldsymbol{m}\left(\omega, S_x\right) = \prod_{j=p-1}^{1} m_j\left(\omega, \mu_{zj}, h_j, S_{zj}, S_x\right) \tag{20}$$

is the transfer matrix through the layers. By combining Eqs. (14) and (19), we obtain

$$\begin{bmatrix} \left(u_y\right)_{p-1} \\ \left(\sigma_{yz}\right)_{p-1} \end{bmatrix} = \begin{bmatrix} \boldsymbol{m}_{11}\left(u_y\right)_0 + \boldsymbol{m}_{12}\left(\sigma_{yz}\right)_0 \\ \boldsymbol{m}_{21}\left(u_y\right)_0 + \boldsymbol{m}_{22}\left(\sigma_{yz}\right)_0 \end{bmatrix}, \tag{21}$$

where $\boldsymbol{m}_{vj}$ are the elements of the matrix $\boldsymbol{m}$. Taking into account the traction-free condition at the upper surface, and assuming that there are no sources at $z = +\infty$, Eq. (21) simplifies to

$$\begin{bmatrix} A_p \\ i\omega S_{zp}\mu_{zp}A_p \end{bmatrix} = \begin{bmatrix} \boldsymbol{m}_{11}\left(u_y\right)_0 \\ \boldsymbol{m}_{21}\left(u_y\right)_0 \end{bmatrix}, \tag{22}$$
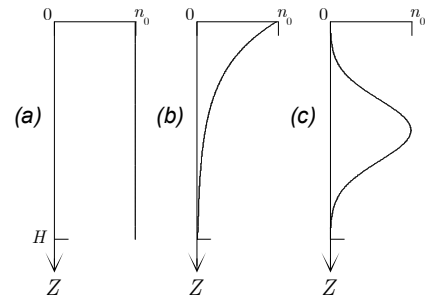
Figure 3. Profiles of the crack density number $n(z)$: (a) uniform; (b) exponential; (c) Gaussian.

which yields to an equation for S_x^2

$$\boldsymbol{m}_{21} = i\omega S_{zp}\mu_{zp}\,\boldsymbol{m}_{11}. \tag{23}$$

This is the Love-wave dispersion equation for p transversely isotropic layers. Although Love waves are surface waves, Eq. (23) contains bulk wave information. In the case of two-layer half-space, $\boldsymbol{m} = m_1$ and Eq. (23) reduces to [1, 8]

$$iS_{z1}\mu_{z1}\tan\omega S_{z1}h_1 = S_{z2}\mu_{z2}. \tag{24}$$

In the long-wave limit, each matrix m_j becomes the identity matrix. Therefore, Eq. (20) reduces to

$$\boldsymbol{m} = \prod_{j=p-1}^{1} m_j = \begin{pmatrix} 1 & 0 \\ 0 & 1 \end{pmatrix}, \tag{25}$$

and the dispersion equation becomes

$$S_{zp}\mu_{zp} = 0, \tag{26}$$

or

$$\operatorname{Re} S_x = s_{zp} \text{ and } \operatorname{Im} S_x = 0. \tag{27}$$

DEPTH-VARYING HALF-SPACE

Suppose that strip-like cracks are randomly distributed under the free surface of in isotropic half-space up to a certain depth H $\left(\gg a\right)$. All the cracks are parallel to the free surface. The disorder inside the damaged region is not uniform but depends on depth.

The depth-varying half-space is discretized into p layers in which the random distribution of the cracks is uniform (*cf.* Figure 1). The surrounding medium is the matrix. In view of the coherent antiplane wave propagation with frequency ω, each *uniformly*-damaged layer may be seen as a transversely isotropic homogeneous layer of the *effective* material. The pth layer is a semi-infinite substrate of the matrix material. For each layer $j = 1, 2, ..., p-1$, $h_j = H/(p-1)$ is the constant thickness and $n(z_j) = n_j$ is the constant number of cracks per unit area. Propagation in each layer is governed by the effective slowness of the coherent shear bulk wave. The elastic parameters of each layer, associated with the coherent antiplane wave motion, are spatially constant but frequency dispersive and complex-valued. According to Eqs (4), (5) and (7) the effective slowness s_{zj} of the coherent shear bulk wave and the effective shear stiffness μ_{zj} depend on the number density of cracks n_j and on the frequency, while ρ_j and μ_{xj} are constant functions. We have

$$\rho_j = \rho_0 \,, \ \mu_{xj} = \mu_0 \,, \ s_{xj} = s_T \,, \ s_{zj}^2\left(\omega, n_j\right) = \frac{\rho_0}{\mu_{zj}\left(\omega, n_j\right)} \,, \quad (28)$$

for $j = 1, 2, \ldots, p-1$ and

$$\rho_p = \rho_0 \,, \ \mu_{xp} = \mu_{zp} = \mu_0 \,, \ s_{xj} = s_{zj} = s_T \,. \quad (29)$$

The dispersion relation for coherent Love-type waves, when the depth-varying distribution of cracks is seen as a stack of effective layers bonded to the substrate, is given by

$$\boldsymbol{m}_{21}\left(\omega, S_x\right) = \mathrm{i}\omega\mu_0\sqrt{s_T^2 - S_x^2}\ \boldsymbol{m}_{11}\left(\omega, S_x\right). \quad (30)$$

Unlike the standard case of Love waves, the effective layer-parameters μ_{zj} and s_{zj} are dispersive and also complex-valued, hence all the solutions S_x of Eq. (30) are generally complex-valued. Equation (30) admits different families of formal solutions related to two Riemann sheets of $S_{zp} = \sqrt{s_T^2 - S_x^2}$. We are concerned only with the Love-type dispersion branches $S_x^{(i)}(\omega)$, $i = 0, 1, \ldots$, which describe waves decaying into the depth of the substrate. Imposing the inequality condition

$$\mathrm{Im}\, S_{zp}^{(i)} = \mathrm{Im}\sqrt{s_T^2 - S_x^{(i)2}} \geq 0 \,, \quad (31)$$

we observe that the found solutions satisfy $\mathrm{Im}\, S_x^{(i)} \geq 0$ (for $\mathrm{Re}\, S_x^{(i)} > 0$ and the axes X, Z as in Figure 2), *i.e.* they also decrease in amplitude along the propagation direction due to the attenuation within the layers.

ATTENUATION DISPERSION CURVES

As an example, Love-type branches are calculated for cracks with width $a = 1$ mm, which are randomly distributed within a region of thickness $H = 15$ mm in an aluminium matrix with $\rho_0 = 2.7$ g/cm^3 and $\mu_0 = 26.45$ GPa.

The results are displayed in terms of the effective phase velocity and the effective attenuation

$$c_x^{(i)} = \mathrm{Re}\left(1 / S_x^{(i)}\right), \ \alpha_x^{(i)} = \omega\,\mathrm{Im}\, S_x^{(i)}, \quad (32)$$

as functions of ωH. In this paper, three profiles of the crack density number $n(z)$ are exemplified, *i.e.*,

uniform: $\qquad n(z) = n_0 \,;$ $\qquad\qquad (33)$

exponential: $\quad n(z) = n_0\exp\left(-\lambda z\right);$ $\qquad (34)$

Gaussian: $\qquad n(z) = n_0\exp\left[-\left(\dfrac{z-H/2}{\sigma}\right)^2\right],$ $\quad (35)$

with $0 \leq z \leq H$, $n_0 = 50\,000$ cracks/m^2, $\lambda = 0.3$ mm and $\sigma = 3$ mm. These profiles are displayed in Figure 3.

Note that the scattering dispersion parameter $\tilde{\omega} = \omega s_T a$ is less than 6 when the frequency is less than 3 MHz (with ωH less than 284 rad.mm/μs).

The non-uniform multi-cracked half-space is viewed as stack of p layers. When the number of layers increases, the difference between the acoustic impedance of each pair of consecutive layers tends to zero. Therefore, the results should converge for a very fine discretization. In the following, the number of layers p is chosen to be equal to 101.
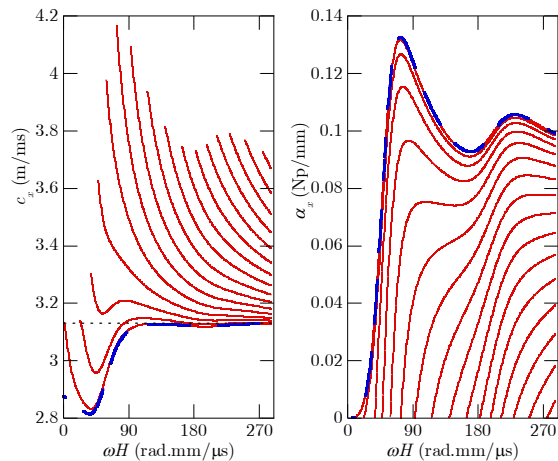
Figure 4. Dispersion branches of the phase velocity $c^{(i)}$ and the attenuation $\alpha^{(i)}$ for the coherent Love-type waves guided by a near-surface *uniform* distribution of cracks (as shown in Fig. 3a). Solid red curves are the dispersion branches; dashed blue curves are the velocity $c(\omega)$ and the attenuation $\alpha(\omega)$ of bulk waves in the *effective* layer material; a dotted horizontal line is the effective phase velocity for the matrix (substrate).
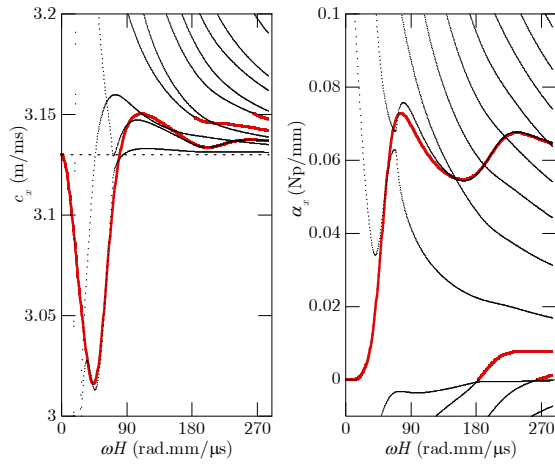
Figures 4-6 show the dispersion branches of the effective phase velocity $c^{(i)}$ and the effective attenuation $\alpha^{(i)}$ for the coherent waves guided by a near-surface distribution of cracks for the crack density profiles shown in Figure 3.

Fundamental branch

Figure 3 shows the Love-type branches calculated for the uniform profile of the crack density (Figure 2a). Note that the dispersion equation (23) for $\left(p-1\right)$ layers of constant thickness $h = H / \left(p-1\right)$ and uniform crack densities n_0 is equivalent to Eq. (24) for the same density number n_0 of cracks, distributed uniformly within a layer of thickness H [1]. The effective velocity $c(\omega)$ and the effective attenuation $\alpha(\omega)$ of coherent shear bulk waves in the *effective* layer material are also displayed in Figure 3.

Starting from high frequency, the fundamental phase-velocity curve $c_x^{(0)}(\omega)$ trails above the bulk-wave effective-velocity in the *effective* layer $c(\omega)$. This is as would be expected for Love waves in a homogeneous layer [8]. However, for the case in hand $c(\omega)$ is dispersive. With increasing frequency the velocity reaches a minimum at $\tilde{\omega} = \mathrm{e}^{-1/2}$ [5] and then curves upwards by approaching the velocity in the matrix from below. Hence so does the branch $c_x^{(0)}(\omega)$. The fundamental branches $c_x^{(0)}$ corresponding to non-uniform profiles of the crack density, Figures 5 and 6, show similar trends, however, with increasing frequency, they oscillate to approach the effective velocity in the matrix from above.

The attenuation curve $\alpha_x^{(0)}(\omega)$ in Figure 4, corresponding to the fundamental branch, is close to the attenuation $\alpha(\omega) = \omega\,\mathrm{Im}\, s_z(\omega)$ of coherent shear bulk waves in the *effective* layer. The later can be considered as an approximation of the fundamental attenuation curve, *i.e.*, $\alpha_x^{(0)}(\omega) \lessgtr \alpha(\omega)$, or vice-versa. In particular, for the case of non-uniform profiles of the crack density, the attenuation curves $\alpha_x^{(0)}(\omega)$ in Figures 5 and 6 might be considered as an approximation of the *effective* attenuation of coherent shear bulk waves in the *depth-varying* distribution of cracks corresponding to Figures 3b and 3c, respectively.

Figure 5. Dispersion branches of the effective phase velocity $c^{(i)}$ and the effective attenuation $\alpha^{(i)}$ for the coherent waves guided by a near-surface *depth-varying* distribution of cracks. The crack density follows an exponential profile, see Fig. 3b. Solid red curves are the dispersion branches; dotted curves are the branches of nonphysical solutions which increase both into the depth and along the propagation direction; a dotted horizontal line is the effective phase velocity for the matrix material (substrate).

Non-fundamental branches

Scattering-induced attenuation underlies an unusual layout of the origin points (cutoffs) of the dispersion curves with $i > 0$. Denote the frequency and velocity at these points by $\overline{\omega}_x^{(i)}$ and $\overline{c}_x^{(i)} \equiv c_x^{(i)}\left(\overline{\omega}^{(i)}\right)$. In the absence of absorption, all the cutoffs lie on the constant line $c_p = c_T$ ($= 3.13$ m/ms) corresponding to the grazing propagation $k_{zp} = \omega S_{zp} = 0$ in the substrate [8]. This is no longer the case due to the layer attenuation. The Love-type branches satisfy the conditions $\operatorname{Im} S_x^{(i)} \geq 0$ and $\operatorname{Im} S_{zp}^{(i)} \geq 0$. For an elastic substrate (with real s_p), $\operatorname{Im} S_x^{(i)}$ and $\operatorname{Im} S_{zp}^{(i)}$ vanish simultaneously. Thus the cutoff points ($\overline{\omega}^{(i)}, \overline{c}^{(i)}$) occur when

$$\operatorname{Im} S_x^{(i)} = 0 \Leftrightarrow \operatorname{Im} S_{zp}^{(i)} = 0, \tag{36}$$

i.e. the imaginary part of the slowness vector s in the substrate turns to zero. Its real part has positive components $\operatorname{Re} S_x^{(i)} = 1 / \overline{c}_x^{(i)}$ and $\operatorname{Re} S_{zp}^{(i)} = -\sqrt{s_p^2 - S_x^{(i)2}}$ whence $\overline{c}_x^{(i)} > c_p$. That is why the cutoff points (36) lie above the substrate velocity c_p.

Beyond the cutoffs, the Love-type velocity and attenuation branches are continued by the branches of non-physical solutions (*i.e.* solutions that are not localized at the surface) with $\operatorname{Im} S_x^{(i)} < 0$ and $\operatorname{Im} S_{zp}^{(i)} < 0$, which increase both into the depth and along the propagation direction. These branches are displayed only in Figures 4 and 5 for clarity.

Figures 4-6 show that the cutoff velocity $\overline{c}_x^{(i)}$ increases for the first few branches and then oscillates around a constant value. It is interesting to note that the envelope curve of cutoff $\overline{c}_x^{(i)}$ has similar shape as the attenuation curve $\alpha_x^{(0)}(\omega)$ corresponding to the fundamental branch.

It is also seen that all the attenuation branches $\alpha_x^{(i)}(\omega)$ with $i > 0$, which start from zero value at the successive cutoff frequencies $\overline{\omega}^{(i)}$ increase with growing ω in a similar manner. The high-frequency extent of all the branches $c_x^{(i)}(\omega)$ approach the limit c_p.
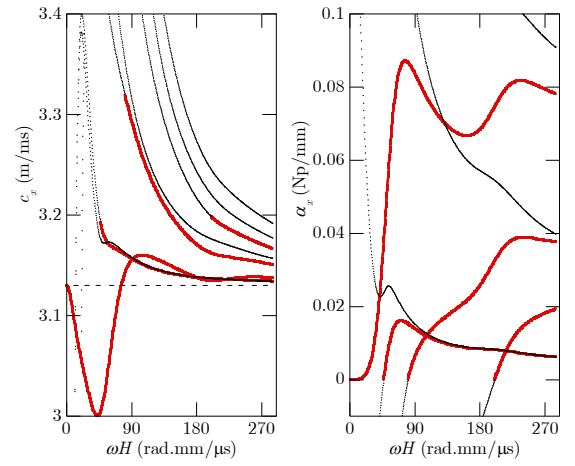
Figure 6. Same as in Figure 5. The crack density follows a Gaussian profile, see Fig. 3c.

CONCLUSION

A dynamic-homogenization approach has been used for calculating the spectrum of coherent antiplane waves in a half-space which contains a random distribution of strip-like cracks within finite depth beneath the surface. The disorder inside the damaged region is not uniform but depends on depth. It is shown that the effect of the dispersion and attenuation caused by the scattering leads to some unusual spectral features such as a curved high-frequency asymptotic of the fundamental branch and supersonic cutoffs of the high-order branches starting above the substrate velocity.

REFERENCES

1   C. Aristégui, A.L. Shuvalov, O. Poncelet, M. Caleap, "Trapping of shear acoustic waves by a near-surface distribution of cavities," *J. Acoust. Soc. Am.* **125**, 628–631 (2009).

2   C. Aristégui, M. Caleap, O. Poncelet, A.L. Shuvalov, Y.C. Angel, "Coherent wave propagation in solids containing spatially varying distributions of finite-size cracks," Ultrasonic Wave Propagation in Non Homogeneous Media, eds. A. Léger et M. Deschamps, Springer Proceedings in Physics **128**, 423–435 (2009).

3   J.-M Conoir, S. Robert, A. El Mouhtadi, F. Luppé, "Reflection and transmission at low concentration by a depth-varying random distribution of cylinders in a fluid slab-like region," *Wave Motion* **46**, 522–538 (2009).

4   M. Caleap and C. Aristégui, "Effective antiplane properties in the presence of frictional shear cracks," *J. Geophys. Res.* **115**, B02302 (2010).

5   Y.C. Angel and Y.K. Koba, "Complex-valued wavenumber, reflection and transmission in an elastic solid containing a cracked slab region," *Int. J. Solids Struct.* **35**, 573–592 (1998).

6   M. Caleap, C. Aristégui, and Y.C. Angel, "Effect of crack opening and orientation on dispersion and attenuation of antiplane coherent wave," *Geophys. J. Int.* **177**, 1151–1165 (2009).

7   N.A. Haskel, "The dispersion of surface waves on multilayered media," *Bull. Seismol. Soc. Am.* **43**, 17–34 (1953).

8   J.L. Rose, *Ultrasonic Waves in Solid Media* (Cambridge U.P., Cambridge, 1999), Chap. 10.